articles

molecular pharmaceutics

cIBR Effectively Targets Nanoparticles to LFA-1 on Acute Lymphoblastic T Cells

Chuda Chittasupho,[†] Prakash Manikwar,[†] Jeffrey P. Krise,[†] Teruna J. Siahaan,[†] and Cory Berkland*[,†,‡]

[†]Department of Pharmaceutical Chemistry, and [‡]Department of Chemical and Petroleum Engineering, The University of Kansas, Lawrence, Kansas, 66047

Received July 30, 2009; Revised Manuscript Received October 26, 2009; Accepted November 2, 2009

Abstract: Leukocyte function associated antigen-1 (LFA-1) is a primary cell adhesion molecule of leukocytes required for mediating cellular transmigration into sites of inflammation via the vascular endothelium. A cyclic peptide, cIBR, possesses high affinity for LFA-1, and conjugation to the surface of poly(DL-lactic-*co*-glycolic acid) nanoparticles can specifically target and deliver the encapsulated agents to T cells expressing LFA-1. The kinetics of targeted nanoparticle uptake by acute lymphoblastic leukemia T cells was investigated by flow cytometry and microscopy and compared to untargeted nanoparticles. The specificity of targeted nanoparticles binding to the LFA-1 integrin was demonstrated by competitive inhibition using free cIBR peptide or using the I domain of LFA-1 to inhibit the binding of targeted nanoparticles. The uptake of targeted nanoparticles was concentration and energy dependent. The cIBR-conjugated nanoparticles did not appear to localize with lysosomes whereas untargeted nanoparticles were detected in lysosomes in 6 h and steadily accumulated in lysosomes for 24 h. Finally, T-cell adhesion to epithelial cells was inhibited by cIBR nanoparticles. Thus, nanoparticles displaying the cIBR ligand may offer a useful targeted drug delivery system as an alternative treatment of inflammatory diseases involving transmigration of leukocytes.

Keywords: LFA-1; leukocytes; peptide; nanoparticles; targeting

1. Introduction

Leukocytes play an important role in disease defense and participate in the adaptive immune response. Under normal conditions, leukocytes circulate between the bloodstream and the lymphatic system as nonadherent cells.[1] Upon receiving signals from inflammatory mediators, various cell adhesion molecules are up-regulated and leukocytes are recruited to the vascular endothelium.[1] Leukocytes selectively accumulate at sites of inflammation via this multivalent adhesion mechanism and subsequently migrate into underlying tissues.[2] Several adhesion molecules mediate the process including members of the integrin family and their immunoglobulin (Ig) superfamily ligands.[1,3] The recruitment of leukocytes from the bloodstream to the inflammatory site involves a multistep adhesion cascade (e.g., tethering, rolling, activation and arrest). The integrins playing a major role during arresting and transmigration are LFA-1, $\alpha_4\beta_1$ and $\alpha_4\beta_7$ which bind to members of the immunoglobulin superfamily

* Corresponding author. Current address: Department of Pharmaceutical Chemistry and Chemical and Petroleum Engineering, 2095 Constant Ave, Lawrence, KS 66047. Phone: (785) 864-1455. Fax: (785) 864-1454. E-mail: berkland@ku.edu.

[†] Department of Pharmaceutical Chemistry.

[‡] Department of Chemical and Petroleum Engineering.

(1) Bechard, D.; Arnaud, S.; Hamida, H.; Thibaut, G.; Anne, T.; Marc, A.; Jöel, P.; Jean-Paul, D.; André-Bernard, T.; Philippe, L. Human Endothelial-Cell Specific Molecule-1 Binds Directly to the Integrin CD11a/CD18 (LFA-1) and Blocks Binding to Intercellular Adhesion Molecule-1. *J. Immunol.* **2001**, *167*, 3099–3160.

(2) Sigal, A.; Bleijs, D. A.; Grabovsky, V.; van Vliet, S. J.; Dwir, O.; Figdor, C. G.; van Kooyk, Y.; Alon, R. The LFA-1 Integrin Supports Rolling Adhesions on ICAM-1 Under Physiological Shear Flow in a Permissive Cellular Environment. *J. Immunol.* **2000**, *165*, 442–452.

(3) Yusuf-Makagiansar, H.; Anderson, M. E.; Yakovleva, T. V.; Murray, J. S.; Siahaan, T. J. Inhibition of LFA-1/ICAM-1 and VLA-4/VCAM-1 as a therapeutic approach to inflammation and autoimmune diseases. *Med. Res. Rev.* **2002**, *22*, 146–167.

10.1021/mp900185u © **2010 American Chemical Society**
Published on Web 11/02/2009

on endothelium such as ICAM-1.[4] In inflammatory diseases, the extravasation of leukocytes into the inflammed tissues ultimately propagates further inflammation which may lead to a chronic disease state. LFA-1 has emerged as an interesting target for treatment of inflammatory diseases and drug delivery.

LFA-1 is constitutively expressed in a low affinity conformation on the plasma membrane of leukocytes.[5] The ligand binding activity of LFA-1 is tightly regulated. LFA-1 activation results from an increase in the affinity for ligand induced by a conformational change, and clustering of integrins on the cell surface.[4] Rolling leukocytes respond to chemokines on vascular endothelial cells by expressing specific receptors that transmit intracellular signals through G proteins.[4] Chemokine receptor signaling changes the conformation of LFA-1 from a closed form (low affinity conformation) on the T-cell surface to an open form (high affinity conformation) and hence enables T cells to adhere and then migrate across the vascular wall. LFA-1 clustering is initiated by lateral migration of integrins to form multivalent binding foci, thus strengthening the adhesion.[6]

Leukocytes express molecules from the β_2 integrin subfamily which includes leukocyte function associated antigen-1 (LFA-1, $\alpha_L\beta_2$, CD11a/CD18), MAC-1 (CD11b/CD18) and P150, 95 (CD11c/CD18). These molecules mediate binding to the intercellular adhesion molecule-1 (ICAM-1) Ig superfamily.[2,3] ICAM-1 (CD54) is the major LFA-1 ligand expressed on endothelial cells, on epithelial cells and on antigen presenting cells (APC). ICAM-1 is upregulated by proinflammatory cytokines such as IL-1, IL-4, IL-6, TNF-α and IFN-γ during inflammation. LFA-1 binds to ICAM-1 via specific interaction between the I domain of LFA-1 and domain 1 (D1) of ICAM-1. Blockade of this molecular interaction using monoclonal antibodies has been shown to be efficacious against acute inflammation,[7] and autoimmune diseases such as diabetes,[8] rheumatoid arthritis[9] and psoriasis[10,11] in addition to suppressing allograft rejection.[12,13]

Here, a small peptide antagonist known to allosterically block binding of ICAM-1 to LFA-1 was used as a targeting ligand for nanoparticles.[14] cIBR (cyclo(1,12)-Pen-PRGGSVLVTGC-OH) is a cyclic peptide derived from D1 of ICAM-1. NMR, docking experiments and competitive inhibition by anti-LFA-1 have shown that the binding site of cIBR is on the I domain of LFA-1.[14−16] cIBR has been characterized to bind to the L site of the I domain of PMA activated LFA-1.[14] This peptide has been shown to interfere with T-cell homotypic and heterotypic adhesion and with mixed lymphocyte reaction.[16−18] Interestingly, cIBR has been reported to be internalized by LFA-1 integrin on the surface of T cells, but not internalized into LFA-1 deficient cell lines,[14,15,19] suggesting that cIBR could be used as a targeting ligand for selective intracellular drug delivery to leukocytes.

LFA-1 mediated adhesion is mediated by integrin clustering in addition to the activation of this receptor. Although

(4) Hogg, N.; Laschinger, M.; Giles, K.; McDowall, A. T-cell integrins: more than just sticking points. *J. Cell Sci.* **2003**, *116*, 4695–4705.

(5) Sarantos, M. R.; Raychaudhuri, S.; Lum, A. F. H.; Staunton, D. E.; Simon, S. I. Leukocyte function-associated antigen 1-mediated adhesion stability is dynamically regulated through affinity and valency during bind formation with intercellular adhesion molecule-1. *J. Biol. Chem.* **2005**, *280*, 28290–28298.

(6) Hogg, N.; Henderson, R.; Leitinger, B.; McDowall, A.; Porter, J.; Stanley, P. Mechanisms contributing to the activity of integrins on leukocytes. *Immunol. Rev.* **2002**, *186*, 164–171.

(7) Guerette, B.; Skuk, D.; Celestin, F.; Huard, C.; Tardif, F.; Asselin, I.; Roy, B.; Goulet, M.; Roy, R.; Entman, M.; Tremblay, J. P. Prevention by anti-LFA-1 of acute myoblast death following transplantation. *J. Immunol.* **1997**, *159*, 2522.

(8) Moriyama, H.; Yokono, K.; Amano, K.; Nagata, M.; Hasegawa, Y.; Okamoto, N.; Tsukamoto, K.; Miki, M.; Yoneda, R.; Yagi, N.; Tominaga, Y.; Kikutani, H.; Hioki, K.; Okumura, K.; Yagita, H.; Kasuga, M. Induction of tolerance in murine autoimmune diabetes by transient blockade of leukocyte function-associated antigen-1/intercellular adhesion molecule-1 pathway. *J. Immunol.* **1996**, *157*, 3737–3743.

(9) Kavanaugh, A. F.; Davis, L. S.; Jain, R. I.; Nichols, L. A.; Norris, S. H.; Lipsky, P. E. A phase I/II open label study of the safety and efficacy of an anti-ICAM-1 (intercellular adhesion molecule-1; CD54) monoclonal antibody in early rheumatoid arthritis. *J. Rheumatol.* **1996**, *23*, 1338–1344.

(10) Papp, K.; Bissonnette, R.; Krueger, J. G.; Carey, W.; Gratton, D.; Gulliver, W. P.; Lui, H.; Lynde, C. W.; Magee, A.; Minier, D.; Ouellet, J. P.; Patel, P.; Shapiro, J.; Shear, N. H.; Kramer, S.; Walicke, P.; Bauer, R.; Dedrick, R. L.; Kim, S. S.; White, M.; Garovoy, M. R. The treatment of moderate to severe psoriasis with a new anti-CD11a monoclonal antibody. *J. Am. Acad. Dermatol.* **2001**, *45*, 665–674.

(11) Gottlieb, A. B.; Krueger, J. G.; Wittkowski, K.; Dedrick, R.; Walicke, P. A.; Garovoy, M. Psoriasis as a model for T-cell-mediated disease: Immunobiologic and clinical Effects of treatment with multiple doses of Efalizumab, an anti-CD11a antibody. *Arch. Dermatol.* **2002**, *138*, 591–600.

(12) Isobe, M.; Yagita, H.; Okumura, K.; Ihara, A. Specific acceptance of cardiac allograft after treatment with antibodies to ICAM-1 and LFA-1. *Science* **1992**, *255*, 1125–1127.

(13) Harihara, Y.; Sugawara, Y.; Inoue, K; Kubota, K.; Bandai, Y.; Makuuchi, M.; Miyasaka, M. Dose dependent immunosuppressive effects of antibodies to ICAM-1 and LFA-1 on hepatic allografts. *Transplant. Proc.* **1996**, *28*, 1794–1795.

(14) Anderson, M. E.; Tejo, B. A.; Yakovleva, T.; Siahaan, T. J. Characterization of Binding Properties of ICAM-1 Peptides to LFA-1: Inhibitors of T-cell Adhesion. *Chem. Biol. Drug Des.* **2006**, *68*, 20–28.

(15) Anderson, M. E.; Siahaan, T. J. Mechanism of binding and internalization of ICAM-1-derived cyclic peptides by LFA-1 on the surface of T cells: a potential method for targeted drug delivery. *Pharm. Res.* **2003**, *20*, 1523–1532.

(16) Zimmerman, T.; Oyarzabal, J.; Sebastián, E. S.; Majumdar, S.; Tejo, B. A.; Siahaan, T. J.; Blanco, F. J. ICAM-1 peptide inhibitors of T-cell adhesion bind to the allosteric site of LFA-1. An NMR characterization. *Chem. Biol. Drug Des.* **2007**, *70*, 347–353.

(17) Tibbetts, S. A.; Seetharama, S. D. J.; Siahaan, T. J.; Benedict, S. H.; Chan, M. A. Linear and cyclic LFA-1 and ICAM-1 peptides inhibit T cell adhesion and function. *Peptides* **2000**, *21*, 1161–1167.

(18) Tibbetts, S. A.; Chirathaworn, C.; Nakashima, M.; Seetharama, S. D. J.; Siahaan, J. T.; Marcia, A. C.; Benedict, H. S. Peptides derived from icam-1 and lfa-1 modulate t cell adhesion and immune function in a mixed lymphocyte culture1. *Transplantation* **1999**, *68*, 685–692.

the mechanism of clustering remains to be clarified,[6] receptor clustering appears to be the consequence of an initial high affinity interaction of LFA-1 with multivalent ICAM-1.[5,6] Multivalent interactions of multiple ligands on nanoparticles can increase the binding avidity by orders of magnitude.[20] In this study, cIBR peptide was conjugated to the surface of nanoparticles to mimic the clustering of ICAM-1 and hence increase the avidity of binding to LFA-1 on T cells. cIBR conjugated nanoparticles (cIBR-NPs) bound to LFA-1 on T cells (Molt-3) more rapidly and to a greater extent compared to untargeted nanoparticles. In addition, cIBR-NPs were shown to block the adhesion of Molt-3 cells to A549 lung epithelial cells. These findings suggest a potential dual therapeutic mechanism for cIBR-NPs to control inflammatory diseases by blocking leukocyte adhesion and by targeting the delivery of drugs (e.g., anti-inflammatory agents).

2. Experimental Section

2.1. Materials. cIBR peptide (cyclo(1,12)-Pen-PRGGS-VLVTGC-OH) (M_w 1,174.5) was synthesized on a Pioneer peptide synthesizer (PerSeptive Biosystems, CA). Poly(DL-lactic-*co*-glycolic acid) (50:50) with terminal carboxyl group (PLGA, inherent viscosity 0.67dL/g, M_w ~90 kDa) was purchased from LACTEL Absorbable Polymers International (Pelham, AL). Pluronic F-127, Texas Red dextran (10,000 kDa, lysine fixable) and 2′,7′-bis-(2-carboxyethyl)-5-(and-6)-carboxyfluorescein, acetoxymethyl ester (BCECF, AM), were purchased from Invitrogen Molecular Probes, Inc. (Carlsbad, CA). Coumarin-6 was obtained from Polysciences, Inc. (Warrington, PA). Dialysis membrane (M_wCO 100,000) was purchased from Spectrum laboratory Products Inc. (Rancho Dominguez, CA). RPMI 1640 medium, A549 cell line and the Molt-3 cell line were obtained from American Type Culture Collection (Manassas, VA). Phorbol 12-myristate 13-acetate (PMA) was purchased from BIOMOL International, L.P. (Plymouth Meeting, PA).

2.2. Methods. *2.2.1. PLGA Nanoparticle Preparation and Characterization.* Nanoparticles encapsulating a fluorescent marker, coumarin-6, were formulated using a solvent displacement method.[21] In brief, PLGA was dissolved in acetone (18 mg/mL) containing coumarin-6 (50 μg/mL). The solution was slowly transferred to a water phase containing 0.1% Pluronic F-127-COOH (25 mL) under mild stirring (300 rpm). Terminal hydroxyl groups on Pluronic F-127 were converted to carboxyl groups according to a reported procedure.[22,23] The nanoparticles spontaneously formed due to the rapid removal of acetone. Excess surfactant was removed by dialysis against a 0.2% mannitol solution for 48 h.

2.2.2. Conjugation of cIBR Peptide to PLGA-Nanoparticles. Pluronic F-127-COOH coated PLGA nanoparticles (2.2 mg/mL) were buffered using 2-(*N*-morpholino)ethanesulfonic acid (MES; pH 6.5). Nanoparticles were then incubated with 100 mM 1-ethyl-3-[3-dimethylaminopropyl]carbodiimide hydrochloride (EDC) and 50 mM *N*-hydroxysulfosuccinimide (sulfo-NHS) for 15 min.[23] The activated carboxyl terminus of Pluronic F127-COOH on the surface of nanoparticles was allowed to react with the amino terminus of the cIBR peptide (170 μmole) for 12 h at room temperature. Conjugated NPs were collected by centrifugation (16089*g*, 10 min) and washed three times with purified water. The size and charge of NPs and cIBR-NPs were characterized using dynamic light scattering (ZetaPALS, Brookhaven Instrument Inc.).

The amount of free cIBR after the reaction was quantified by gradient reversed phase HPLC (SHIMADZU) using a C_{18} column. The HPLC consisted of a SCL-10A SHIMADZU system controller, LC-10AT VP SHIMADZU liquid chromatograph, SIL-10A XL SHIMADZU autoinjecter set at 10 μL injection volume, DGU-14A SHIMADZU degasser, sample cooler, and SPD-10A SHIMADZU UV−vis detector (220 nm). The HPLC−UV system was controlled by a personal computer equipped with SHIMADZU class VP Software. All separations were carried out using a Vydac HPLC protein and peptide C_{18} column. Gradient elution was carried out at constant flow of 1 mL/min, from 100% A to 0% A (corresponding to 0% B to 100% B) for 15 min, followed by an isocratic elution at 100% B for 3 min. Mobile phase compositions were (A) acetronitrile−water (5:95) with 0.1% TFA and (B) acetonitrile−water (90:10, v/v) with 0.1% trifluoroacetic acid (TFA). At the end of each analysis, the cartridge was re-equilibrated at 1 mL/min flow rate for 13 min with A. The density of peptide on the surface of nanoparticles was calculated from the total surface area assuming a normal Guassian particle size distribution.

2.2.3. Stimulation of LFA-1 by Phorbol 12-Myristate 13-Acetate (PMA). The Molt-3 cell line (1×10^6 cells/mL) was stimulated using 0.4 μM of PMA for 20 h. According to previous reports, PMA is able to activate LFA-1 and improve binding to ICAM-1.[24] Cells at the same concentration were not activated and used as a control. Molt-3 cells, with or without PMA stimulation, were incubated with anti-LFA-1-FITC (0, 0.05, and 0.1 mg/mL) at 4 °C for 45 min.

(19) Gürsoy, R. N.; Siahaan, J. T. Binding and internalization of an ICAM - 1 peptide by the surface receptors of T cells. *J. Pept. Res.* **1999**, *53*, 414–421.

(20) Hong, S.; Leroueil, P. R.; Majoros, I. J.; Orr, B. G.; Baker, J. R., Jr.; Holl, M. M. B. The binding avidity of a nanoparticle-based multivalent targeted drug delivery platform. *Chem. Biol.* **2007**, *14*, 107–115.

(21) Avgoustakis, K. Pegylated poly(Lactide) and poly(Lactide-Co-Glycolide) nanoparticles:preparation, properties and possible applications in drug delivery. *Curr. Drug Delivery* **2004**, *1*, 321–333.

(22) Guerrouache, M.; Karakasyan, C.; Gaillet, C.; Canva, M.; Millot, M. C. Immobilization of a functionalized poly(ethylene glycol) onto β-cyclodextrin-coated surfaces by formation of inclusion complexes: application to the coupling of proteins. *J. Appl. Polym. Sci.* **2006**, *100*, 2362–2370.

(23) Chittasupho, C.; Xie, S.; Baoum, A.; Yakovleva, T.; Siahaan, J. T.; Berkland, C. ICAM-1 targeting of doxorubicin-loaded PLGA nanoparticles to lung epithelial cells. *Eur. J. Pharm. Sci.* **2009**, *37*, 141–150.

Free antibodies were removed by rinsing three times with PBS after centrifugation (595*g*, 1.5 min). The fluorescent intensity of cells was analyzed by flow cytometry. In addition, the specificity of anti-LFA-1-FITC was confirmed by incubation with A549 cells, which express ICAM-1 but not LFA-1. A549 were cultured as previously reported.[23] Molt-3 cells coexpress LFA-1 and ICAM-1. Both cells were incubated with 0.4 μM of PMA at 37 °C for 20 h. Anti-LFA-1-FITC (0.05 mg/mL) was incubated with Molt-3 cells for 45 min at 4 °C. Cells were washed three times with PBS and centrifuged (595*g*, 1.5 min) The fluorescent intensity of Molt-3 cells was determined by using a FACscan flow cytometer. Data analysis was performed using Cell Quest software (BD).

2.2.4. Binding and Uptake of cIBR-NPs into Molt-3 Cells. The binding and uptake of cIBR-NP encapsulated fluorescent dye was studied by using flow cytometry. PMA stimulated Molt-3 cells (1×10^6 cells/mL) were added in a 96 well-plate (200 μL/well) containing $CaCl_2$ (1.5 mM) and incubated with cIBR-NPs or NPs encapsulating coumarin-6 (2.2 mg/mL, 90 μL) at 37 °C for 5, 15, 20, and 35 min. Cells were then repeatedly centrifuged (460*g*, 4 °C for 1 min) and washed three times with cold PBS and fixed with 4% paraformaldehyde. The fluorescent intensity of cells was measured using the FACscan flow cytometer. Data analysis was performed using Cell Quest software (BD). To investigate whether the uptake was dependent on the nanoparticle concentration, Molt-3 cells (1×10^6 cells/mL, 100 μL) in serum free medium were added to a 96 well-plate containing $CaCl_2$ (1.5 mM) followed by incubation with cIBR-NPs (70 μL/well) at 37 °C for 30 min at various concentrations (0.08, 0.16, 0.33, 0.66, 1.31, 2.63, 5.25, and 10.50 mg/mL). Cells were washed three times with cold PBS by centrifugation at 460*g*, 4 °C for 1 min. The fluorescent intensity of the Molt-3 cells was again determined using the FACscan flow cytometer. Data analysis was performed as before.

2.2.5. Inhibition of the Binding of cIBR-NPs. cIBR-NPs were hypothesized to bind to the I domain of LFA-1, a binding site of cIBR peptide.[14−16] The binding site of cIBR-NPs was studied by blocking with cIBR. LFA-1 on Molt-3 (4×10^4 cells/mL) was stimulated by PMA (0.4 μM) for 20 h. Cells were added to a 96-well plate (100 μL) containing $CaCl_2$ (1.5 mM). Free cIBR at various concentrations (0.0, 0.31, 0.63, 1.2, and 2.5 mg/mL, 80 μL) was incubated with cells for 40 min at 4 °C to inhibit the binding of cIBR-NPs or NPs to LFA-1. Cells were then incubated with cIBR-NPs or untargeted NPs (2.2 mg/mL, 80 μL) at 4 °C for 40 min. Cells were rinsed three times with cold PBS by centrifugation (460*g*, 1 min, 4 °C), fixed with 4% paraformaldehyde and again analyzed by flow cytometry .

To further investigate whether the binding site of cIBR-NPs is LFA-1 I domain or not, free LFA-1 I domain was used to block the binding of cIBR-NPs to LFA-1 on plasma membrane of Molt-3 cells. The LFA-1 I domain was dissolved in water at various concentrations, 0, 0.31, 0.63 1.25 and 2.50 mg/mL, and was mixed with cIBR-NPs (2.1 mg/mL, 80 μL) at 37 °C for 1 h. After incubation, Molt-3 cells (1×10^6 cells/mL) were added (100 μL) into the mixture and incubated at 37 °C for 40 min. Cells were pelleted by centrifugation (460*g*, 1 min, 4 °C), and free cIBR-NPs and the I domain were removed by three centrifugation/washing cycles. Cells were fixed using 4% paraformaldehyde. The binding of cIBR-NPs to the cells was determined from the fluorescent intensity analyzed by flow cytometry using the specified data analysis.

Inhibition of cIBR-NP uptake was also investigated by incubating BSA (0, 0.31, 0.63, 1.25 and 2.50 mg/mL) with cIBR-NP (2.1 mg/mL, 80 μL) at 37 °C for 1 h. Albumin is known to adsorb to hydrophobic particle surfaces and was used here to determine if albumin could nonspecifically block ligand interactions with receptors. After incubation, Molt-3 cells (1×10^6 cells/mL) were added (100 μL) into the mixture and incubated at 37 °C for 40 min to allow binding of cIBR-NP to LFA-1 of cells. Free cIBR-NP and BSA were washed three times with PBS. Cells were fixed with 4% paraformaldehyde. The binding of cIBR-NP to the cells was determined from the fluorescent intensity analyzed by flow cytometry.

2.2.6. Temperature Effects on the Binding and Internalization of cIBR-NPs and NPs. The energy-dependent internalization of cIBR-NPs into Molt-3 cells was investigated in this study. LFA-1 on Molt-3 cells (1.1×10^6 cells/mL) were activated by PMA (0.4 μM) for 20 h at 37 °C, and cells were then added to a 96-well plate (100 μL/well) and incubated with serum free medium containing 1.5 mM $CaCl_2$ for 40 min at 4 and 37 °C followed by incubation with cIBR-NPs or NPs (2.2 mg/mL, 90 μL/well) for 5, 15, 25, 35, and 45 min. Cells were then washed three times with PBS and fixed with 4% paraformaldehyde. The uptake of cIBR-NPs or NPs by cells was determined from the fluorescent intensity analyzed using flow cytometry as before.

2.2.7. Fluorescence Microscopy of the Uptake of cIBR-NPs by Molt-3 Cells. Fluorescence microscopy was performed to compare the extent of binding and uptake of cIBR-NPs and untargeted NPs in Molt-3 cells. Molt-3 cells (1×10^6 cells/mL) were activated by using 0.4 μM PMA for 24 h. Cells were then added to an 8-well plate containing $CaCl_2$ (1.5 mM). cIBR-NPs or NPs (2.2 mg/mL) were incubated with the cells for 5, 15, 30 min and 1 h at 37 °C, 5% CO_2. Unbound nanoparticles were removed by washing three times with cold PBS and fixed with 4% paraformaldehyde. Fluorescence micrographs were acquired using the FITC filter set of a Nikon Eclipse 80i microscope equipped for epifluorescence. Micrographs were captured using an Orca ER camera (Hamamatsu, Inc., Bridgewater, NJ) and analyzed by Metamorph, version 6.2 (Universal Imaging Corp., West Chester, PA).

2.2.8. Lysosomal Trafficking of cIBR-NPs in Molt-3 Cells. Fluorescence microscopy was utilized to investigate the intracellular fate of cIBR-NPs and untargeted NPs in

(24) Tominaga, T.; Sugie, K.; Hirata, M.; Morii, N.; Fukata, J.; Uchida, A.; Imura, H.; Narumiya, S. Inhibition of PMA-induced, LFA-1-dependent lymphocyte aggregation by ADP ribosylation of the small molecular weight GTP binding protein, rho. *J. Cell Biol.* **1993**, *>120*, 1529–1537.

Molt-3 cells. Molt-3 cells (1×10^6 cells/mL) were activated with 0.4 μM PMA for 20 h. Cells were washed and dispersed in Texas Red dextran (M_w 10,000, lysine fixable, 1 mg/mL) in serum free medium and incubated for 2 h at 37 °C, 5% CO_2. Cells were washed three times with serum free medium. Cells were then incubated in serum free medium at 37 °C, 5% CO_2 for 12 h to allow the dye to traffic lysosomes. Cells were then added to an 8-well plate containing $CaCl_2$ (1.5 mM). Then cIBR-NPs or NPs (100 μL, 2.2 mg/mL) were added to cells and incubated for 10 min at 37 °C, 5% CO_2. Unbound nanoparticles were removed by washing three times with serum free medium. Cells were then incubated in serum free medium for each time period (30 min, 1 h, 2 h, 3 h, 4 h, 6 h, 8 h and 24 h.). Cells were washed by centrifugation at 856*g* for 1 min and fixed with 4% paraformaldehyde. Fluorescence emissions of nanoparticles and lysosomes were observed using FITC and rhodamine filter sets, respectively (Nikon Eclipse 80i microscope equipped for epifluorescence). Micrographs were captured using an Orca ER camera (Hamamatsu, Inc.). Colocalization of nanoparticles with lysosomes was analyzed by Metamorph, version 6.2.

2.2.9. Inhibition of Heterotypic Adhesion by cIBR-NPs. cIBR-NPs were hypothesized to bind to LFA-1 of Molt-3 cells, hence blocking the binding of LFA-1 of Molt-3 cells and ICAM-1 of A549 lung epithelial cells. The inhibition of LFA-1 and ICAM-1 adhesion by cIBR-NPs was monitored in this study. A549 cells (8×10^5 cells/mL) were incubated with TNF-α (1,000 U/mL) for 48 h to activate the expression of ICAM-1 as reported previously.[23] LFA-1 on Molt-3 cells was activated by 0.4 μM of PMA in serum free medium for 20 h. Molt-3 cells were labeled with a fluorescent dye, 2′,7′-bis-(2-carboxyethyl)-5-(and-6)-carboxyfluorescein, acetoxymethyl ester (BCECF, AM) (5 μL, 2 mM), in 20 mL of PBS for 15 min at 37 °C. Cells were washed three times with PBS and resuspended in 5 mL of PBS (final concentration of cells was 5.5×10^5 cells/mL). Molt-3 cells were then transferred to a 96-well plate (200 μL/well) and incubated with various concentrations of cIBR-NPs (0, 0.38, 0.75, and 1.50 mg/mL) at 37 °C for 30 min. Molt-3 cells were then transferred to A549 culture on 8-well plates to evaluate the interaction between ICAM-1 on A549 cells and LFA-1 on Molt-3 cells at 37 °C, 5% CO_2 for 45 min. After incubation, unbound Molt-3 cells were washed away with cold PBS three times and the culture was fixed with 4% paraformaldehyde. The binding of Molt-3 to A549 cells was quantified by counting the bound Molt-3 in four images taken with the Nikon Eclipse 80i microscope.

2.2.10. Statistical Analysis. Statistical evaluation of data was performed using an analysis of variance (one-way ANOVA). Newman−Keuls was used as a posthoc test to assess the significance of differences. To compare the significance of the difference between the means of two groups, a *t* test was performed; in all cases, a value of $p < 0.05$ was accepted as significant.

Table 1. Nanoparticle Properties at Specified Formulation Points[a]

	effective diameter (nm) [mean ± SD]	polydispersity [mean ± SD]	zeta potential value (mV) [mean ± SD]
NP	199 ± 8.0	0.08 ± 0.04	−22.5 ± 1.4
cIBR-NP	248 ± 10	0.08 ± 0.05	−25.7 ± 1.8

[a] Values are representative of three experiments.

3. Results

3.1. PLGA Nanoparticle Preparation and Characterization. PLGA nanoparticles were prepared using a solvent displacement method.[23] Nanoparticles were formed from PLGA, which served as a hydrophobic core to encapsulate the poorly water-soluble dye, coumarin-6.[23] The diameter of nanoparticles was approximately 200 nm with a low polydispersity suggesting a narrow size distribution. Modified Pluronic F-127 bearing carboxylic acid termini yielded negatively charged NPs. The zeta potential value was about −23 mV (Table 1). It is probable that the strong negative charge provided some electrostatic stabilization to reduce agglomeration and maintain particle size. Furthermore, free carboxylic acid groups on the modified surfactant allowed conjugation of the targeting peptide.

3.2. Conjugation of cIBR Peptide to PLGA Nanoparticles. The cIBR peptide was covalently attached to the carboxylic acid end groups of modified Pluronic F-127 on the nanoparticle surface using carbodiimide chemistry.[23] The conjugation efficiency was determined by quantifying the unconjugated ligand remaining in the reaction medium after nanoparticle separation. The amount of cIBR peptide conjugated on NP measured by RP-HPLC increased during the reaction (0−20 h) (Figure 1A). The peptide density on the surface of nanoparticles after reaction was calculated assuming a normal Guassian particle size distribution (Table 2).[23] The conjugation reaction was also performed in the absence of EDC to observe any possible adsorption (electrostatic or hydrophobic interaction) of cIBR peptide to the nanoparticles. The result showed that the adsorption of peptide was negligible since the amount of peptide conjugated with NP analyzed by RP-HPLC did not increase when peptide was incubated with nanoparticles without activation of COOH (Figure 1B).

3.3. PMA Stimulates Aggregation of Molt-3 Cells. Molt-3 cells were found to aggregate in response to PMA (Figure 2A). Although a small amount of homotypic adhesion of Molt-3 cells also occurred in the absence of PMA, PMA stimulated Molt-3 cells exhibited much larger cell clusters. In previous reports, PMA was shown to increase the avidity of LFA-1 via *rho*A protein which works as an intracellular transducer of protein kinase C activation leading to integrin activation and cell aggregation.[24] Immunofluorescence flow cytometry showed that the expression of LFA-1 on Molt-3 cells was not changed when incubated with PMA, suggesting that PMA did not induce expression of LFA-1 (Figure 2B). This result was previously observed in other LFA-1 bearing

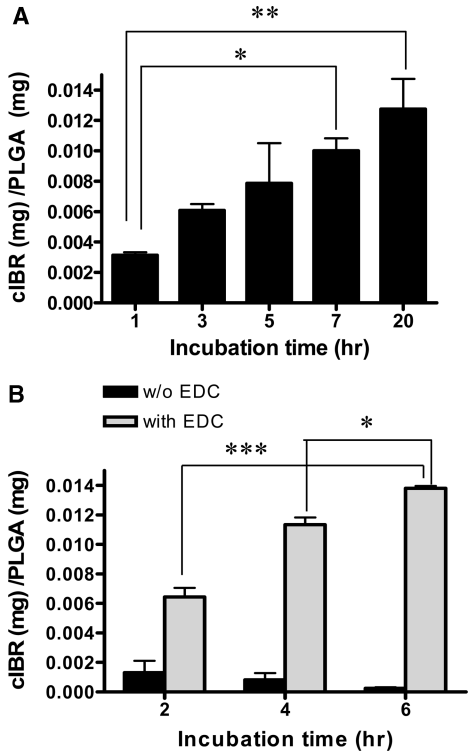

Figure 1. (A) Measurement of cIBR peptide reacted with nanoparticles over time. The amount of cIBR peptide conjugated on the nanoparticle surface increased with incubation time indicating reaction to nanoparticles. (B) The amount of peptide on the nanoparticle was constant when the reaction was performed without EDC. Data are presented as mean ± SD ($n = 3$); *** indicates $p < 0.001$, ** indicates $p < 0.01$ and * indicates $p < 0.05$.

Table 2. Density of cIBR on the Surface of PLGA Nanoparticles[a]

	size (nm)	total surface area (m^2/g of PLGA)	surface cIBR (pmol/cm^2)
cIBR-NP	248	18.1	39.0 ± 9.6

[a] Values are representative of three experiments (mean ± SD).

cells.[25] As a control, A549 lung carcinomic epithelial cells, expressing ICAM-1, but not LFA-1 were incubated with PMA and also incubated with anti-LFA-1-FITC. The fluorescent intensity measured by flow cytometry was negligible compared with Molt-3 cells since A549 cells lack LFA-1 (Figure 2C).

3.4. cIBR-NPs Exhibit Interaction with Molt-3 Cells. The binding and uptake of cIBR-NPs by Molt-3 cells were monitored using flow cytometry. The interaction of cIBR-NPs and Molt-3 cells was substantially greater than that of untargeted NPs (Figure 3). Molt-3 cells showed ~5-fold higher fluorescence when incubated with targeted nanoparticles. The fluorescent intensity of Molt-3 cells increased with

(25) Rothlein, R.; Springer, T. A. The requirement for lymphocyte function-associated antigen 1 in homotypic leukocyte adhesion stimulated by phorbol ester. *J. Exp. Med.* **1986**, *163*, 1132–1149.

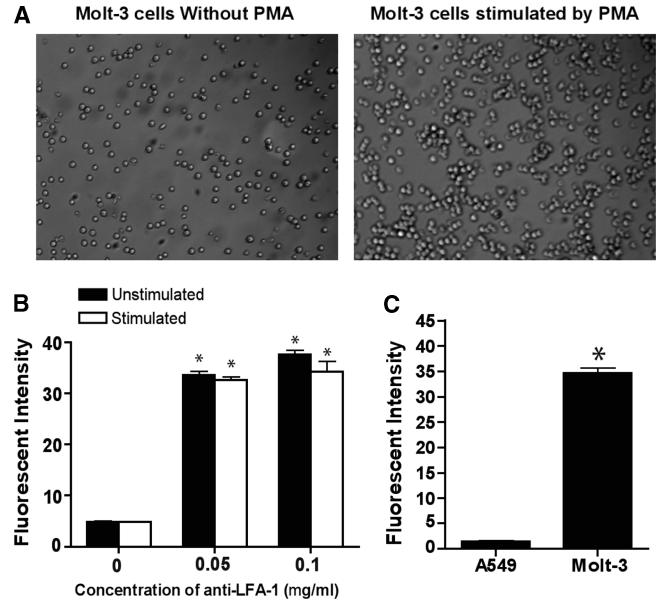

Figure 2. (A) Stimulation of LFA-1 on Molt-3 cells by PMA. Aggregation of PMA stimulated Molt-3 cells was evident compared to unstimulated Molt-3 cells. (B) Binding of anti-LFA-1 to LFA-1 on stimulated and unstimulated LFA-1. Anti-LFA-1-FITC labeling of LFA-1 revealed that the expression of LFA-1 was unchanged for PMA-stimulated compared to unstimulated Molt-3 cells. (C) Negligible fluorescent intensity of anti-LFA-1-FITC was observed when incubated with cells lacking LFA-1 (A549 cells). Data are presented as mean ± SD ($n = 3$); * indicates $p < 0.001$ compared to 0 mg/mL of anti-LFA-1-FITC.

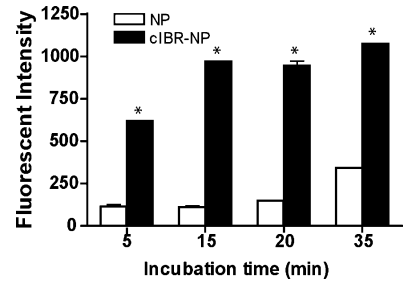

Figure 3. Binding of cIBR-NP to Molt-3 cells. cIBR-NP interaction with Molt-3 cells was significantly greater than untargeted NPs at all time points. The fluorescence of Molt-3 cells incubated with cIBR-NPs increased with time. Data are presented as mean ± SD ($n = 3$); * indicates $p < 0.001$.

time for both particle types but to a larger extent for cIBR-NPs. These results suggested that cIBR-NPs bound to Molt-3 cells more quickly and to a greater extent when compared to untargeted NPs. Furthermore, the binding of cIBR-NPs was also concentration dependent; uptake increased with increasing nanoparticle concentration (Figure 4).

3.5. Free cIBR and the LFA-1 I Domain Inhibited the Binding of cIBR-NPs to Molt-3 Cells. Inhibition of cIBR-NPs was investigated by incubating Molt-3 cells with free cIBR peptide followed by incubation with cIBR-NPs

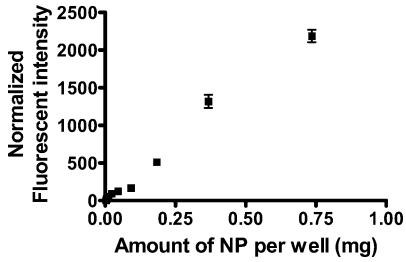

Figure 4. The dependence of cIBR-NP concentration on the binding to Molt-3 cells. The normalized fluorescence of Molt-3 cells increased as the concentration of cIBR-NPs increased.

or NPs. The fluorescent intensity of cells incubated with cIBR-NPs decreased significantly compared to cells incubated with untargeted NPs (Figure 5A). Disrupting of the binding of cIBR-NPs to Molt-3 cells by cIBR peptide suggested cIBR-NPs targeted LFA-1. The binding of untargeted NPs was again very low.

To further validate binding specificity, cIBR-NPs were allowed to bind to the I domain of LFA-1 prior to incubation with Molt-3 cells. The I domain was expected to bind to cIBR on targeted NPs and block the binding of targeted NPs to LFA-1 on Molt-3 cells. As the concentration of the LFA-1 I domain increased, the binding of cIBR-NPs correspondingly decreased (Figure 5B). The binding of cIBR-NPs was reduced to ~60% when 2.5 mg/mL of the I domain was used with cIBR-NPs compared to the absence of the I domain whereas there was no significantly reduction when the same concentration of BSA was added with cIBR-NP (Figure 5C). This result further supported the specific binding of cIBR-NPs to the I domain of LFA-1. Previous reports verified that cIBR peptide has a PRGG sequence with a β-turn structure similar to the D_1 of ICAM-1, the binding site of LFA-1.[14,15] Furthermore, Anderson and Siahaan elucidated the binding specificity of cIBR peptide and showed that cIBR-FITC binding to soluble LFA-1 can be competitively inhibited by an anti-CD11a antibody as an indicator of specific binding of cIBR to the I domain of LFA-1.[14] This binding specificity appeared to be maintained when conjugated to the surface of PLGA nanoparticles.

3.6. Uptake of cIBR-NPs Is Temperature Dependent. Molt-3 cells were incubated with cIBR-NPs at 4 and 37 °C to determine the effect of temperature on the uptake of nanoparticles and to learn whether the mechanism of cIBR-NPs entry into Molt-3 cells was energy dependent. The uptake of cIBR-NPs decreased significantly at 4 °C (Figure 6A), suggesting that cIBR-NPs uptake was indeed energy dependent. Furthermore, the fluorescent intensity of cells incubated with cIBR-NPs at 37 °C increased over time. At low temperature, cIBR-NPs binding was similar to binding at 37 °C; however, the increase in fluorescent intensity occurred more slowly, suggesting that endocytosis was slowed at low temperature. The dependence of temperature on the uptake of untargeted nanoparticles was also investigated. The uptake of nanoparticles without peptide was also decreased at low temperature but to a lesser extent (Figure 6B), confirming an energy dependent endocytic process observed previously.[26]

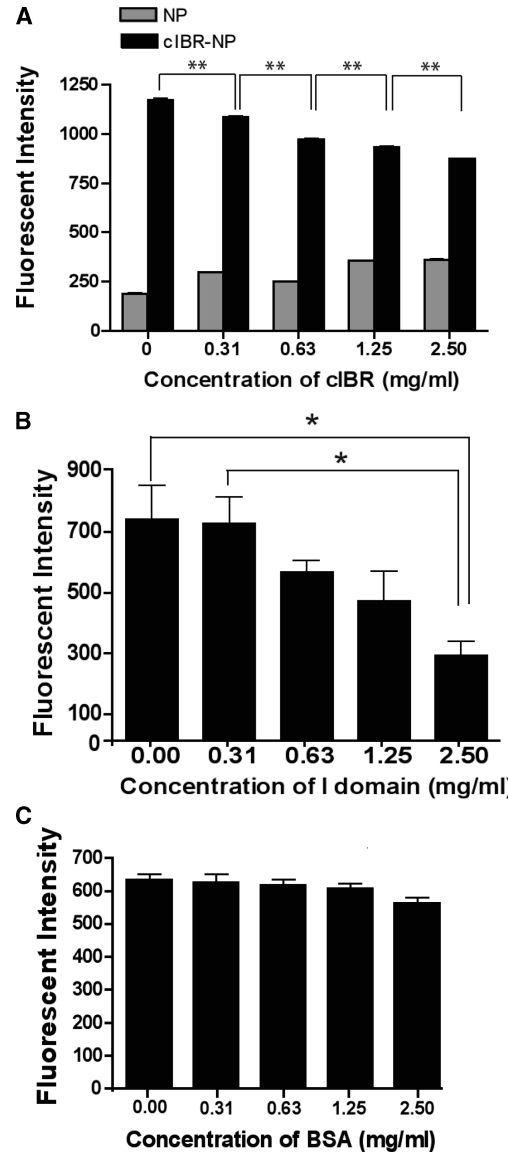

Figure 5. (A) The inhibition of cIBR peptide to the binding of cIBR-NP to Molt-3 cells. The interaction of cIBR-NPs with Molt-3 cells decreased as free cIBR peptide concentration increased, suggesting that cIBR competitively inhibits binding to LFA-1 on Molt-3 cells. Data are presented as mean ± SD (n = 3); ** indicates $p < 0.001$. (B) The inhibition of LFA-1 I domain to the binding of cIBR-NP to Molt-3 cells. The interaction of cIBR-NPs with Molt-3 cells was also competitively inhibited by the I domain of LFA-1. The I domain was added to the NPs prior to addition of cells. Data are presented as mean ± SE (n = 3); * indicates $p < 0.05$. (C) The uptake of cIBR-NP pretreated with BSA by Molt-3 cells did not decrease in the presence of BSA.

(26) Panyam, J.; Labhasetwar, V. Dynamics of endocytosis and exocytosis of Poly(D, L-lactic-co-glycolide) nanoparticles in vascular smooth muscle cells. *Pharm. Res.* **2003**, *20*, 212–220.

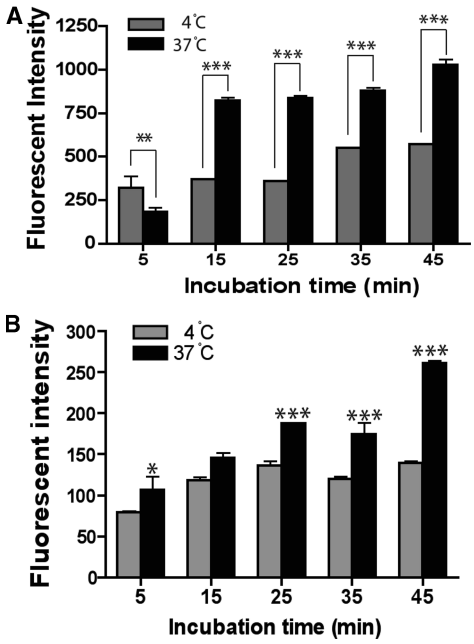

Figure 6. The dependence of temperature on the binding of cIBR-NP to Molt-3 cells. The binding and uptake of (A) cIBR-NPs and (B) NPs were slowed at low temperature (4 °C), which suggested energy dependent endocytosis of nanoparticles. Data are presented as mean ± SD ($n = 3$); * indicates $p < 0.05$, ** indicates $p < 0.01$ and *** indicates $p < 0.001$.

3.7. Fluorescence Microscopy of Molt-3 Cells and Nanoparticles. The uptake of cIBR-NPs and NPs by Molt-3 cells was examined by fluorescence microscopy. The association of cIBR-NPs and NPs with Molt-3 cells was clearly demonstrated by fluorescence micrographs. The fluorescent intensity of cells incubated with untargeted NPs was far less than that of cells incubated with targeted NPs (Figure 7). The fluorescent intensity of cells incubated with NPs slowly increased with incubation time and showed the greatest intensity at the longest time, whereas the fluorescent intensity of cells incubated with cIBR-NPs was quite high initially. These results supported the kinetics of cIBR-NPs incubated with Molt-3 cells determined by flow cytometry. Both suggest the rapid binding and internalization of cIBR-NPs and may suggest receptor saturation.

3.8. Trafficking of cIBR-NPs. Lysosomes are acidic and contain hydrolytic enzymes where nanoparticles and/or encapsulated drugs may be degraded. To investigate whether cIBR-NPs trafficked to the lysosomes or not, fluorescent colocalization studies of lysosomes and nanoparticles were conducted. The lysosomal compartments of Molt-3 cells were stained with Texas Red dextran (lysine fixable) to track cIBR-NPs and NPs uptake. Then, cells were treated with cIBR-NPs or NPs encapsulating the green fluorescent dye. The intracellular localization of nanoparticles was tracked at different time points, and lysosomal accumulation was indicated by yellow fluorescence in merged images (Figure 8). The colocalization of cIBR-NPs with lysosomal vesicles may be not evident over 24 h. The colocalization of untargeted NPs with lysosomes was detectable at 6 h and

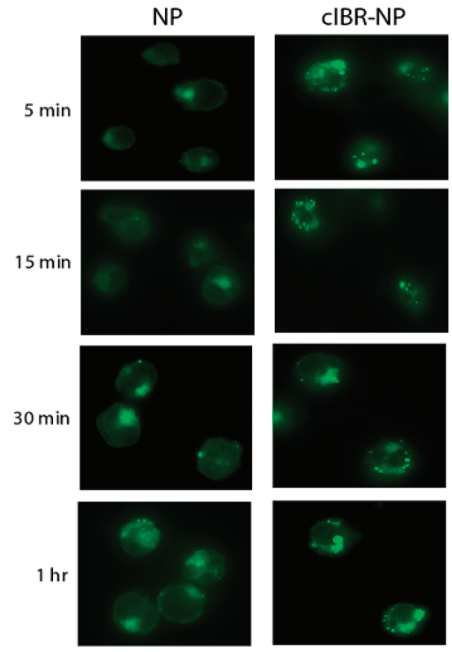

Figure 7. Micrograph of Molt-3 cells incubated with cIBR-NP or NP encapsulating fluorescence dye. Interaction of cIBR-NPs with Molt-3 cells occurred more quickly and to a greater extent compared to untargeted NPs at each incubation time as shown by fluorescence micrographs.

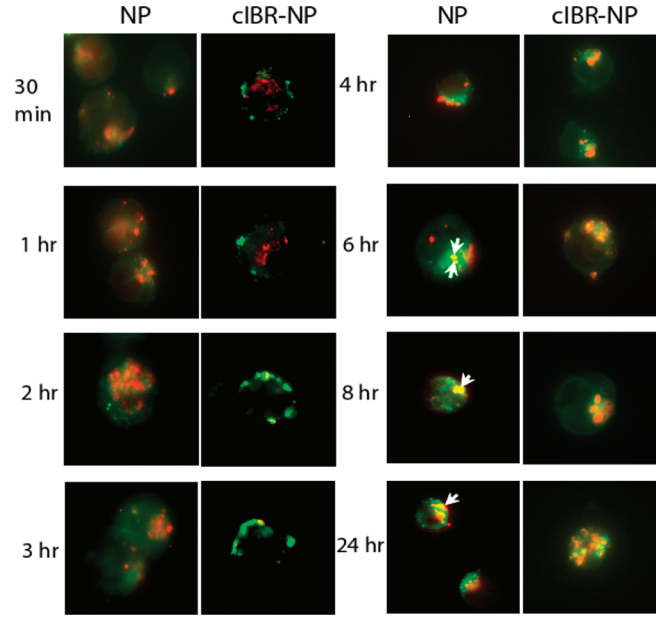

Figure 8. Micrographs of Molt-3 cells incubated with cIBR-NP or NP in the presence of Texas Red dextran. Intracellular trafficking of cIBR-NPs and NPs (green) to lysosomal compartments (red) of Molt-3 cells. The colocalization (yellow fluorescence) of cIBR-NPs with lysosomes was generally not observed over 24 h, whereas colocalization of NPs with lysosomes was first observed at 6 h and slowly increased over 24 h.

was detected until at least 24 h. These results implied that cIBR-NPs did not persist in lysosomes but untargeted NPs slowly accumulated in lysosomes.

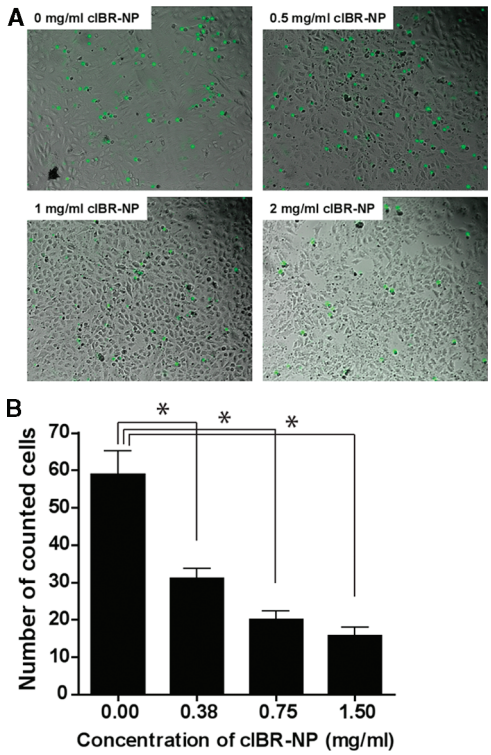

Figure 9. The inhibition of cIBR-NP to the interaction of LFA-1 and ICAM-1 on Molt-3 cells and A549 cells. (A) Optical micrographs of the adhesion of Molt-3 cells (green) to A549 lung epithelial cells at various concentrations of cIBR-NPs. (B) cIBR-NPs inhibited the heterotypic adhesion of Molt-3 cells to A549 cells in a dose dependent manner. Data are presented as mean ± SD ($n = 3$); * indicates $p < 0.001$ compared with 0 mg/mL of cIBR-NPs.

3.9. cIBR-NPs Inhibit the Adhesion of Molt-3 Cells and Lung Epithelial Cells. Leukocyte recruitment to endothelial and epithelial tissues requires interaction of LFA-1 and ICAM-1.[14,27] cIBR peptide alone has been shown to inhibit homotypic and heterotypic cell interactions via binding LFA-1.[17,19,28] The interaction of LFA-1 on PMA-stimulated Molt-3 cells and ICAM-1 expressed on lung carcinomic epithelial cells activated with TNF-α resulted in heterotypic cell adhesion and was investigated by fluorescence microscopy. Micrographs allowed quantification of the number of adhered Molt-3 cells (stained with a green fluorescent dye) to A549 cells (Figure 9A). Pretreatment of Molt-3 cells with cIBR-NPs was investigated as a means to inhibit this heterotypic cell adhesion. When PMA-stimulated Molt-3 cells were preincubated with cIBR-NPs, significant inhibition was observed (Figure 9B). Pretreatment of Molt-3 cells with cIBR-NPs yielded up to a ~73% decrease in adhered cells, suggesting that cIBR-NPs bound to LFA-1 of Molt-3 cells blocked the availability of LFA-1 integrins to bind to ICAM-1 on A549 cells. Furthermore, cIBR-NPs may decrease the availability of LFA-1 on the cell surface via endocytosis of this receptor.[14] The result of this study revealed the potential of cIBR-NPs to inhibit lymphocyte recruitment during inflammatory responses.

4. Discussion

The interaction of LFA-1 and ICAM-1 plays a vital role in leukocyte recruitment and migration across the vasculature during normal leukocyte circulation through lymph nodes and during recruitment in the response to inflammatory signals. LFA-1 also participates in the "immunological synapse" between T lymphocytes and antigen presenting cells (APC).[6] In recent decades, potential therapeutic agents used to block the binding of LFA-1 to ICAM-1 to treat immunological and inflammatory disorders have focused on monoclonal antibodies and small molecules designed to antagonize interactions between these proteins.[29,30] However, hypersensitivity reactions and unpredictable half-lives are often encumbrances for immunotherapy using monoclonal antibodies.[28,30,31] In comparison to monoclonal antibodies, cyclic peptides have been shown to offer improved safety, physicochemical stability and may even improved selectivity to the targeted site.[3,32]

cIBR, a cyclic peptide derived from domain 1 of ICAM-1, has demonstrated specific binding to isolated LFA-1 and to the surface of T cells.[9,10] Previous research showed that cIBR conjugated to the fluorescent dye FITC entered cells via endocytosis; however, cIBR conjugated to doxorubicin mainly passively diffused through the cell membrane of HL-60 cells.[28] Passive diffusion of cIBR-doxorubicin may be a result of the increased hydrophobicity of the conjugate, a change in the conformation of the cIBR peptide after conjugation and/or steric hindrance of doxorubicin at the recognition site of the cIBR peptide.[28] Regardless, these findings suggested that the delivery of some drugs may be improved if the drugs were encapsulated.

In the present study, cIBR was conjugated to the surface of PLGA nanoparticles. The physical incorporation of drug

(27) Porter, J. C.; Hall, A. Epithelial ICAM-1 and ICAM-2 regulate the egression of human T cells across the bronchial epithelium. *FASEB J.* **2009**, *23*, 493–502.

(28) Majumdar, S.; Kobayashi, N.; Krise, J. P.; Siahaan, T. J. Mechanisms of internalization of an ICAM-1 derived peptide by human leukemic cell line HL-60: Influence of physicochemical properties on targeted drug delivery. *Mol. Pharmaceutics* **2007**, *4*, 749–758.

(29) Kelly, T. A.; Jeanfavre, D. D.; McNeil, D. W.; Woska, J. R., Jr.; Reilly, P. L.; Mainolfi, E. A.; Kishimoto, K. M.; Nabozny, G. H.; Zinter, R.; Bormann, B.; Rothlein, R. Cutting edge: A small molecule antagonist of LFA-1-mediated cell adhesion. *J. Immunol.* **1999**, *163*, 5173–5177.

(30) Wofsy, D. Strategies for treating autoimmune disease with monoclonal antibodies. *West. J. Med.* **1985**, *143*, 804–809.

(31) Huang, M.; Matthews, K.; Siahaan, T. J.; Kevil, C. G. α_L-Integrin I domain cyclic peptide antagonist selectively inhibits T cell adhesion to pancreatic islet microvascular endothelium. *Am. J. Physiol.* **2005**, *288*, G67–G73.

(32) Yusuf-Makagiansar, H.; Makagiansar, I. T.; Hu, Y.; Siahaan, T. J. Synergistic inhibitory activity of α- and β-LFA-1 peptides on LFA-1/ICAM-1 interaction. *Peptides* **2001**, *22*, 1995–1962.

in the particle matrix may mask the hydrophobicity of the drug and mitigate potential off-target passive diffusion into cells driven by the poorly water-soluble compound. Furthermore, the grafting of cIBR to the end of a long chain surfactant on the nanoparticle surface can reduce steric hindrance at the cIBR binding site which may have occurred in a single drug−peptide conjugate.[28]

The importance of multivalency in the LFA-1/ICAM-1 interaction and the activation of high avidity LFA-1 in some types of LFA-1 expressing cells have been reported.[33] LFA-1 is exclusively expressed on leukocytes, but these cells do not adhere to ICAM-1 unless activated (e.g., by PMA).[6,34] Furthermore, Welder et al. have demonstrated that monovalent, soluble intercellular cell adhesion molecule-1 (sICAM-1) shows only modest binding to LFA-1 expressed on cells unless it is first rendered multivalent by coupling to polystyrene microspheres, thus, illustrating the importance of multivalency.[35] Pyszniak et al. have demonstrated that sICAM-1-coated microspheres specifically bind to activated LFA-1 but not to the low avidity state.[34] The distribution of high avidity LFA-1 on the cell surface was observed to be highly localized on some types of LFA-1 expressing cells, whereas the low avidity state was more evenly distributed. They also reported that, only after activation with PMA, isolated splenic T cells and murine T-cell hybrodoma T28 bound the sICAM-1 microspheres and the binding was inhibited by anti-LFA-1 mAb. Therefore, utilizing a high density of cIBR ligands on nanoparticles may improve binding efficiency of cIBR-NPs to activated LFA-1 due to multivalent ligand receptor interactions.

When compared to untargeted nanoparticles, grafting cIBR peptide to biodegradable PLGA nanoparticles increased selectivity, the rate, and the extent of binding and internalization by activated LFA-1 on acute lymphoblastic leukemia T cells (Molt-3). The uptake of targeted nanoparticles was concentration and temperature dependent, suggesting receptor-mediated endocytosis. The partial inhibition of nanoparticle uptake at low temperature (4 °C) suggested that the internalization of the cIBR-NPs likely occurred via an energy dependent endocytic pathway.

Lysosomes are acidic intracellular compartments that contain a variety of hydrolytic enzymes. Texas Red dextran is internalized by fluid phase endocytosis and accumulates in lysosomes due to its acid hydrolase-resistant nature.[36] The fate of nanoparticles was investigated by studying the colocalization of nanoparticles and lysosomes via fluorescence microscopy. There was no colocalization of cIBR-nanoparticles and lysosomes was observed suggesting that LFA-1 targeted nanoparticles do not traffic to lysosomes suggesting that LFA-1 targeted nanoparticles do not traffic to lysosomes. The internalization and recycling of LFA-1 to the plasma membrane has been reported.[37] The exocytosis cycle of several types of integrins has also been shown in polymorphonuclear cells including neutrophils.[37] The recycling process of integins is functional to retrieve these receptors and, as they cleave their ligands, to recycle them as adhesion molecules on the plasma membrane.[37] It is possible that cIBR-NPs bound to LFA-1 may enter this receptor recycling process.[37] Regardless, cIBR-NPs may have advantages over untargeted NPs for drug delivery because they can avoid hydrolytic degradation in lysosomes.

5. Conclusion

Targeted drug delivery has emerged as an important strategy to improve the efficacy and reduce the adverse effects of drugs. In the present study, cIBR-NPs were characterized as a potential drug delivery system targeting the receptor, LFA-1 integrin, on leukocytes. cIBR-NPs were bound and internalized by LFA-1 on Molt-3 T cells much more rapidly and to a greater extent than untargeted nanoparticles. Furthermore, cIBR-NPs bound specifically to LFA-1 on the Molt-3 cell line as confirmed by competitive inhibition assays. cIBR-NPs did not appear to traffic to lysosomal compartments, suggesting that encapsulating drugs in this type of NPs may offer some protection from lysosomal degradation. The adhesion between T cells and lung epithelial cells expressing LFA-1 and ICAM-1, respectively, was significantly inhibited by cIBR-NPs. These studies suggest the plausibility of using LFA-1 as a target molecule with the potential of a dual therapeutic effect by blocking leukocyte recruitment and targeting immunomodulators or anti-inflammatory drugs to leukocytes.

Acknowledgment. The authors acknowledge Prof. Jeffrey Krise for providing the fluorescence microscope. We would like to acknowledge support from the Royal Thai Government, the Coulter Foundation, and the Higuchi Biosciences Center as well as additional lab funding from the American Heart Association, the NIH (R03 AR054035, P20 RR016443 and T32 GM08359-11) and the Department of Defense. In addition, we acknowledge the support of the NSF (CHE 0719464).

MP900185U

(33) Tanaka, Y. Activation of leukocyte function-associated antigen-1 on adult T cell leukemia cells. *Leuk. Lymphoma* **1999**, *36*, 15–23.

(34) Pyszniak, A. M.; Welder, C. A.; Takei, F. Cell surface distribution of high-avidity LFA-1 detected by soluble ICAM-1 coated microspheres. *J. Immunol.* **1993**, *152*, 5241.

(35) Welder, C. A.; Lee, D. H. S.; Takei, F. Inhibition of cell adhesion by microspheres cpated with recombinant soluble ICAM-1. *J. Immunol.* **1993**, *150*, 2203–2210.

(36) Hirota, Y.; Masuyama, N.; Kuronita, T.; Fujita, H.; Himeno, M.; Tanaka, Y. Analysis of post-lysosomal compartments. *Biochem. Biophys. Res. Commun.* **2004**, *314*, 306–312.

(37) Fabbri, M.; Meglio, S. D.; Gagliani, M. C.; Consonni, E.; Molteni, R.; Bender, J. R.; Tacchetti, C.; Pardi, R. Dynamic partitioning into lipid rafts controls the endo-exocytic cycle of the αL/β2 integrin, LFA-1, during leukocyte chemotaxis. *Mol. Biol. Cell* **2005**, *16*, 5793–5803.